Article

Role of Delayed Nonsynaptic Neuronal Plasticity in Long-Term Associative Memory

Ildikó Kemenes,[1] Volko A. Straub,[1,3]
Eugeny S. Nikitin,[1] Kevin Staras,[1,4] Michael O'Shea,[1]
György Kemenes,[1,2,*] and Paul R. Benjamin[1,2,*]
[1] Sussex Centre for Neuroscience
Department of Biological and Environmental Sciences
School of Life Sciences
University of Sussex
Falmer, Brighton BN1 9QG
United Kingdom

Summary

Background: It is now well established that persistent nonsynaptic neuronal plasticity occurs after learning and, like synaptic plasticity, it can be the substrate for long-term memory. What still remains unclear, though, is how nonsynaptic plasticity contributes to the altered neural network properties on which memory depends. Understanding how nonsynaptic plasticity is translated into modified network and behavioral output therefore represents an important objective of current learning and memory research.
Results: By using behavioral single-trial classical conditioning together with electrophysiological analysis and calcium imaging, we have explored the cellular mechanisms by which experience-induced nonsynaptic electrical changes in a neuronal soma remote from the synaptic region are translated into synaptic and circuit level effects. We show that after single-trial food-reward conditioning in the snail *Lymnaea stagnalis,* identified modulatory neurons that are extrinsic to the feeding network become persistently depolarized between 16 and 24 hr after training. This is delayed with respect to early memory formation but concomitant with the establishment and duration of long-term memory. The persistent nonsynaptic change is extrinsic to and maintained independently of synaptic effects occurring within the network directly responsible for the generation of feeding. Artificial membrane potential manipulation and calcium-imaging experiments suggest a novel mechanism whereby the somal depolarization of an extrinsic neuron recruits command-like intrinsic neurons of the circuit underlying the learned behavior.
Conclusions: We show that nonsynaptic plasticity in an extrinsic modulatory neuron encodes information that enables the expression of long-term associative

*Correspondence: g.kemenes@sussex.ac.uk (G.K.); p.r.benjamin@sussex.ac.uk (P.R.B.)
[2] These authors contributed equally to this work.
[3] Present address: Department of Cell Physiology and Pharmacology, Faculty of Medicine and Biological Sciences, University of Leicester, Leicester LE1 9HN, United Kingdom.
[4] Present address: Medical Research Council Laboratory for Molecular and Cell Biology, University College London, London WC1E 6BT, United Kingdom.

memory, and we describe how this information can be translated into modified network and behavioral output.

Introduction

It is now widely accepted that nonsynaptic as well as synaptic plasticity are substrates for long-term memory [1–4]. Although information is available on how nonsynaptic plasticity can emerge from cellular processes active during learning [3], far less is understood about how it is translated into persistently modified behavior. There are, for instance, important unanswered questions regarding the timing and persistence of nonsynaptic plasticity and the relationship between nonsynaptic plasticity and changes in synaptic output. In this paper we address these important issues by looking at an example of learning-induced nonsynaptic plasticity (somal depolarization), its onset and persistence, and its effects on synaptically mediated network activation in an experimentally tractable molluscan model system.

Unlike previous studies investigating nonsynaptic plasticity (reviewed in [3]), we used a single-trial associative learning paradigm to induce long-term memory. This allowed a precise temporal analysis of nonsynaptic electrical changes after learning and made it possible to relate these changes to various postacquisition stages of memory formation at the behavioral and neural levels. This was not possible with multitrial learning paradigms, used in previous work investigating learning-induced nonsynaptic plasticity in molluscan feeding systems [5–7]. Moreover, we have isolated the learning-induced nonsynaptic change to a neuron that is extrinsic to the synaptic network directly responsible for the generation of the conditioned and unconditioned behavior. This allowed us to examine the contribution of nonsynaptic plasticity to the conditioned response independently of any synaptic changes that might occur in the circuit generating the behavior. In other examples, nonsynaptic plasticity was shown to occur in neurons that are directly responsible for the generation of both the unconditioned and conditioned behavior, making it difficult to determine the independent contributions of nonsynaptic and synaptic plasticity to altered network output [6–11].
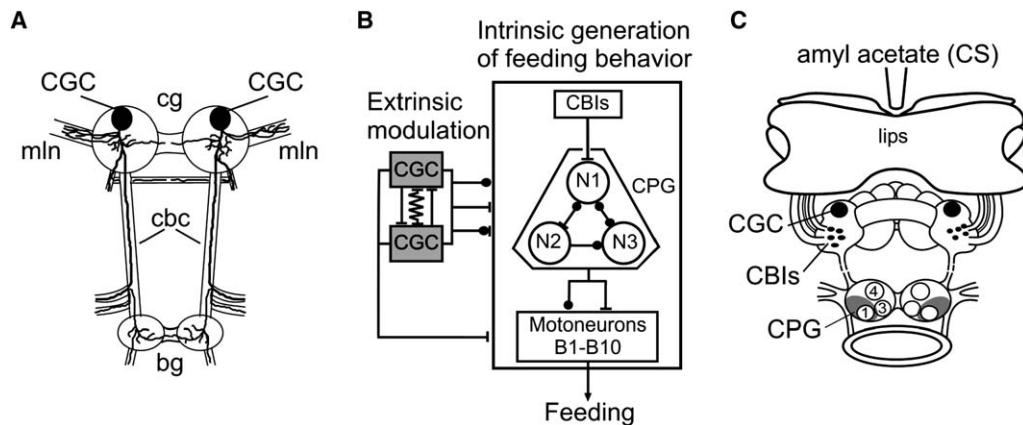
Here, we target identified extrinsic modulatory neurons, known in *Lymnaea* as the cerebral giant cells (CGCs, Figure 1A). These paired serotonergic giant neurons and their homologs in other molluscs (e.g., *Aplysia* [12]) play a permissive role in feeding behavior ([13, 14] and Figure 1B) but have no direct role in the generation of the rhythmic feeding motor pattern [13–16]. By performing electrophysiological analyses in semi-intact preparations (Figure 1C), we show that in animals subjected to a single pairing of amyl-acetate (the CS) with sucrose (the US), the CGCs have a more positive membrane potential than in unpaired control animals. The depolarization is sufficient to increase the network response to the CS, emerges between 16 and 24 hr

Figure 1. Location and Axonal Branching Pattern of the Extrinsic Modulatory Cerebral Giant Cells and Their Synaptic Connections to the Intrinsic Circuit that Generates Feeding Motor Behavior in *Lymnaea*

(A) The paired (left and right) CGCs send their main axon branches into the buccal ganglia (bg) via the cerebro-buccal connectives (cbc) and have side branches within the cerebral ganglia. Their main sensory inputs from the lips are from the median lip nerves (mln). The axonal branching pattern shown here is based on preparations (n > 10) in which both CGCs were intrasomatically filled with the Alexa Fluor 488 dye (Molecular Probes, Leiden, The Netherlands).

(B) The electrically and chemically coupled CGCs provide widespread monosynaptic inputs to the buccal feeding central pattern generator (CPG) and motoneurons. Phasic modulatory cerebral-buccal interneurons (CBIs), CPG interneurons (types N1, N2, and N3), and motoneurons (types B1–B10, some of which also have CPG properties [54]), intrinsic to the feeding network, are primarily responsible for the generation of the rhythmic motor pattern underlying feeding. The CGCs have an extrinsic, state-setting or permissive function in feeding [13, 14].

(C) The semi-intact preparation that allows chemosensory stimulation of the lips, intracellular recording from the CGCs and intrinsic neurons of the feeding network (see Figures 2–5), and extracellular recording of CBI activity from the cbc (see Figure 8). The CPG neurons are located in the gray areas in the buccal ganglia. The interneurons (CGC, CBIs) and motoneurons (B1, B3, B4) recorded in the present work are labeled on the left side of the diagram only. –/\/\/\–, electrotonic synapse; I—, excitatory connection; •—, inhibitory connection, I•—, biphasic, excitatory/ inhibitory connection.

postconditioning, and persists as long as the long-term memory. The depolarization of the CGC soma spreads to local axonal regions and increases the strength of CGC postsynaptic responses. Depolarization of the CGC also leads to an increase in presynaptic calcium levels, a mechanism by which presynaptic depolarization can regulate synaptic function [17]. At the network level, we show that CGC depolarization increases the spike response to the CS in feeding command interneurons, leading to the activation of feeding. These experiments reveal a novel mechanism that links nonsynaptic plasticity occurring outside a behavioral network to modified output arising within the network.

Results

Single-Trial Conditioning Leads to Long-Term Memory and Persistent Depolarization of an Extrinsic Modulatory Interneuron

First, we examined whether single-trial conditioning leads to electrophysiological changes in the CGCs concomitant with the formation of protein synthesis-dependent long-term (>24 hr) memory [18]. The CGCs were chosen as our primary target in these experiments because they provide extrinsic modulation to the feeding system (Figure 1B), and we hypothesized that changes in their electrical properties might support long-term memory in isolation from synaptic network effects directly responsible for the generation of the learned behavior.

About 400 animals were subjected to either a paired or an unpaired single-trial food-reward conditioning protocol [19, 20]. Randomly selected groups of trained (paired protocol) and control (unpaired protocol) snails were

tested for their behavioral feeding response to the CS (amyl-acetate) at 1, 2, 3, 7, or 14 days after conditioning (Figure 2A). At each time point, the trained animals responded significantly (at least $p < 0.05$, Figure 2A) more strongly to the CS than the controls, indicating associative learning.

The membrane potentials of the CGCs in semi-intact lip-CNS preparations (Figure 1C) made from randomly selected trained and control animals also were recorded at each time point. The CGC membrane potential was significantly (at least $p < 0.05$, Figure 2B) different between the trained and control groups on each day of the investigation (Figure 2B).

We also measured CGC input resistance, spike frequency, threshold, amplitude, duration, and after-hyperpolarization that might have been affected by conditioning. We found no significant differences between the trained and control groups in these electrical parameters at any of the time points (data not shown, example traces from the Day 14 experiment are shown in Figure 2B).

Next, we focused our attention to the pre-24 hr period after training. Behavioral tests of intact animals at 2 hr, 4 hr, 6 hr, and 12–16 hr after training (n = between 17 and 23 snails per group) revealed a significant conditioned response (at least $p < 0.05$, Figure 3A) but no significant differences in the CGC membrane potential between preparations from control and trained animals (Figure 3B). So the persistent depolarization has an onset of between 16 hr and 24 hr posttraining, and therefore it is not associated with early memory expression or with the initial steps in long-term memory formation.

In the same experiments, at each time point we also measured CGC input resistance, spike frequency,

A Conditioned response
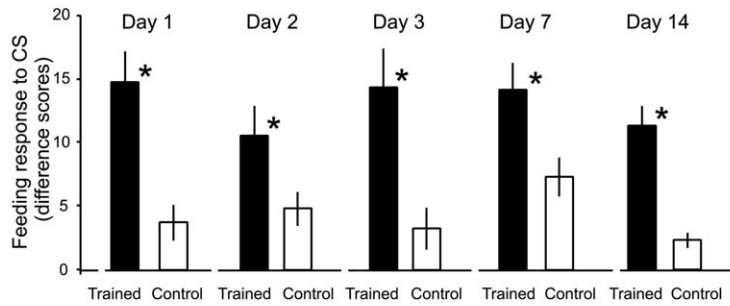
B Membrane potential and other electrical parameters of the CGC
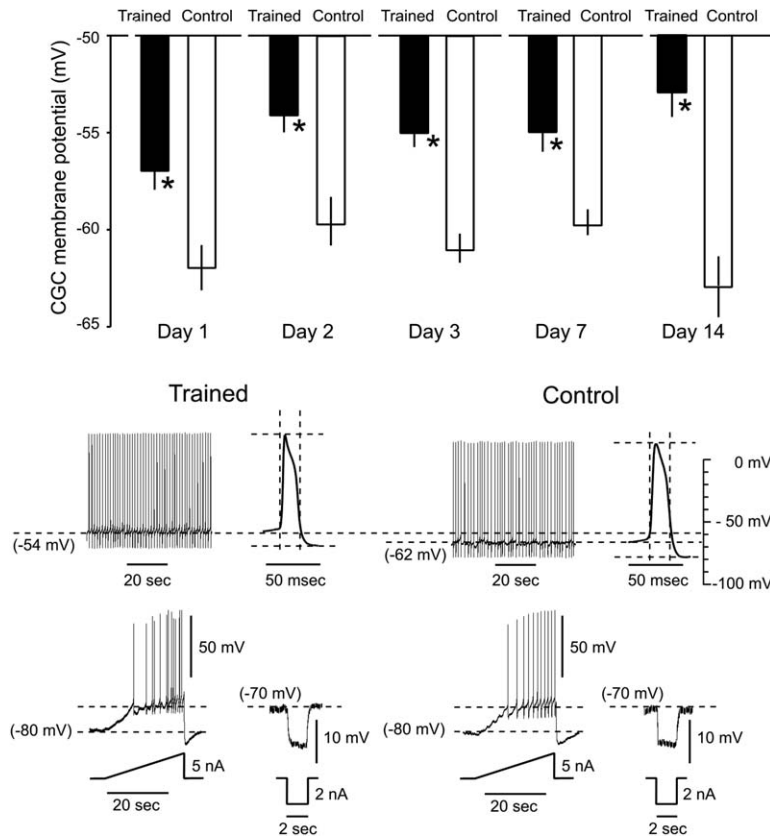
Figure 2. Time Course of Behavioral Changes and Membrane Depolarization of the CGCs 1–14 Days after Single-Trial Classical Conditioning

(A) A significant conditioned response is expressed throughout the 14 day test period. At each time point, pairwise statistical comparisons (unpaired t tests) were made between the CS-evoked feeding response of the trained (mean feeding difference scores between 10.4 and 14.1, n = between 14 and 20 per group) and the control (mean feeding difference scores between 2.3 and 7.3, n = between 13 and 20 per group) groups. No comparisons were planned between the conditioned or control responses at different time points and therefore no ANOVA and post-hoc multiple comparisons were performed. Error bars represent the standard error of the mean (SEM). The computed values for the t test statistics were as follows: Day 1, df = 28, t = 3.9, p < 0.001; Day 2, df = 25, t = 2.2, p < 0.04; Day 3, df = 28, t = 3.2, p < 0.03; Day 7, df = 36, t = 2.5, p < 0.02; Day 14, df = 38, t = 5.1, p < 0.01.

(B) The CGCs are significantly more depolarized in the trained (mean membrane potential values between −53 and −57 mV, n = between 14 and 24 per group) versus the control preparations (mean membrane potential values between −59 and −63 mV, n = between 15 and 26 per group) throughout the same test period. Error bars represent SEM. The computed values for the t test statistics were as follows: Day 1, df = 46, t = 3.0, p < 0.004; Day 2, df = 31, t = 2.5, p < 0.02; Day 3, df = 49, t =3.7, p < 0.0005; Day 7, df = 27, t = 3.2, p < 0.003; Day 14, df = 38, t = 5.1, p < 0.01. Example CGC traces are shown from a preparation from a trained animal (recorded membrane potential, −54 mV) and a control animal (recorded membrane potential, −62 mV) from Day 14 posttraining. Despite the difference in membrane potential, there are no differences between the CGCs from the trained and control animal in spike shape (averaged from 100 s long sections of the CGC traces at recorded membrane potential), spike threshold (ramp depolarization from −80 mV), and input resistance (cells held at −70 mV, averaged voltage responses to five 2 nA hyperpolarizing current pulses are shown).

threshold, duration, amplitude, and after-hyperpolarization. No training-associated changes were detected in any of these parameters within this experiment or between this and the previous experiment (data not shown).

Persistent Depolarization of the CGCs Is Concomitant with the Electrophysiological Expression of the Long-Term Memory Trace

After finding both behavioral memory expression (CS-induced feeding) and CGC depolarization at >24 hr post-training, in a new experiment we tested whether the CGC depolarization is also concomitant with a CS-induced fictive feeding response, the electrophysiological expression of the memory trace. Fictive feeding is defined as the occurrence of rhythmic motoneuronal activity known to be driven by the feeding CPG (N1, N2, and N3 type neurons, Figure 1B).

In the initial behavioral training experiment, the behavioral feeding difference score of the conditioned snails (n = 37) 14 days after the training was 11.2 ± 1.5, significantly (p < 0.001) higher than the difference score of the control animals (2.3 ± 0.6, n = 34). Similarly, when the fictive feeding responses to the CS in semi-intact preparations made from conditioned animals (mean difference score, 3.2 ± 0.8, n = 10) were compared with those in preparations made from unpaired controls (0.5 ± 0.6, n = 10), they were found to be significantly (p < 0.01) greater (Figure 4A). In the example shown in Figure 4B, the CS produced a train of fictive feeding bursts in both the motoneuron recorded here (B4) and the intrinsic feeding command interneuron CV1a, indicative of a conditioned response. By contrast, in the control preparation, only a single delayed burst was recorded in the motoneuron (B3) and only subthreshold inputs were recorded in CV1a (Figure 4C). Replicating

A Conditioned response
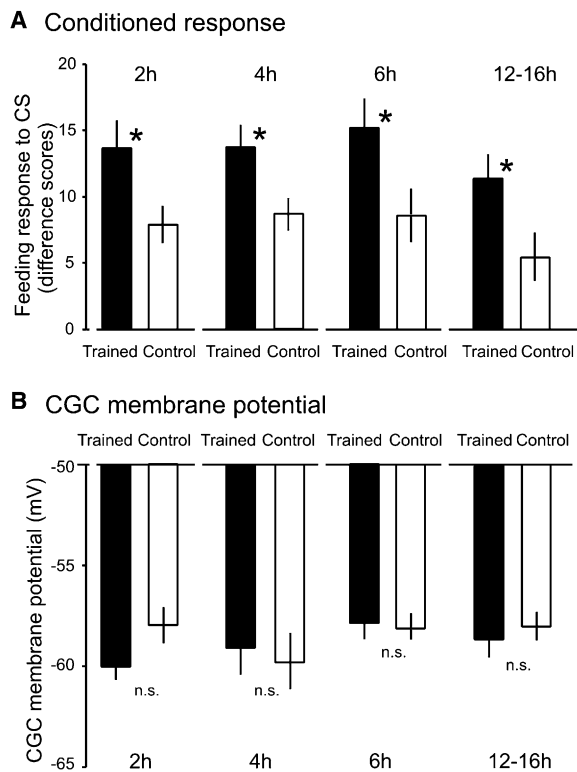

B CGC membrane potential

Figure 3. Behavioral Memory with No Corresponding Electrophysiological Changes in the CGCs 2–16 hr after Single-Trial Classical Conditioning

(A) A conditioned response is expressed throughout the 16 hr test period. Error bars represent SEM. The computed values for the statistics (unpaired t tests) at each time point were as follows: 2 hr, df = 33, t = 2.2, p < 0.003; 4 hr, df = 38, t = 2.4, p < 0.002; 6 hr, df = 37, t = 2.3, p < 0.03; 12–16 hr, df = 40, t = 2.2, p < 0.05.

(B) There is no significant difference in the CGC membrane potential in the trained and the control preparations throughout the same test period (2 hr, df = 14, t = 1.1, p = 0.30; 4 hr, df = 14, t = 0.5, p = 0.65; 6 hr, df = 13, t = 0.7, p = 0.5; 12–16 hr, df = 13, t = 0.24, p = 0.8). Error bars represent SEM.

the result of the previous experiment (Figure 2B), the mean membrane potential of the CGCs in the trained preparations (e.g., Figure 4B) was depolarized (−53 ± 1.3 mV) compared with controls (−63 ± 1.6 mV, unpaired t test, df = 18, t = 4.96, p < 0.001, e.g., Figure 4C). In the same preparations, we found no difference in the baseline firing frequencies of CGCs from conditioned versus unpaired control groups (0.83 ± 0.02 and 0.70 ± 0.07 Hz, respectively), nor was there a significant difference in the CS-evoked spike frequency in the two types of preparations (conditioned, 0.84 ± 0.05 Hz; unpaired control, 0.74 ± 0.07 Hz).

Depolarization of the CGCs Is Sufficient for an Increased Fictive Feeding Response to the Conditioned Stimulus

To establish whether the change in membrane potential is sufficient to enable an enhanced fictive feeding response to the CS, we artificially depolarized the CGCs in naive animals. The membrane potential of CGCs in semi-intact preparations made from naive animals was artificially set to the mean depolarization level that was

found in trained animals from the previous 14 day post-training experiments (−53 mV) and compared with the CS response at control membrane potential (−63 mV) in the same preparations.

Depolarization of the CGC membrane potential to −53 mV with maintained injected current increases the baseline firing rates of the CGCs. However, the previous experiment showed no increase in baseline CGC firing rates in preparations from trained animals compared to preparations from unpaired controls. For this reason, the baseline firing rates at both the control (−63 mV) and depolarized membrane potential levels (−53 mV) were entrained to 1 Hz throughout the experiment by injecting brief suprathreshold current pulses through a second electrode. The experiment therefore tested the ability of the membrane potential depolarization alone to influence the strength of the fictive feeding response to the CS.

When the CGCs were depolarized to −53 mV, naive preparations (n = 12) showed an increased response to amyl-acetate (Figure 5). The fictive feeding response was significantly (p < 0.01) stronger (difference score, 2.0 ± 0.7) when the CGC's membrane potential was set to −53 mV than when it was set to −63 mV (Figure 5A, difference score, −0.25 ± 0.3; examples are shown in Figures 5B and 5C). This result shows that CGC depolarization alone is sufficient to produce a significant increase in fictive feeding response to the CS. The learning-induced depolarization of the CGCs demonstrated in the previous experiment (Figure 4) therefore appears to make a significant contribution to long-term memory by enabling the activation of the conditioned behavior by the CS. This conclusion was supported by statistical analysis showing that there was no significant difference between CS-induced fictive feeding rates observed in conditioned animals (3.2 ± 0.8, Figure 4A) versus those observed when the CGCs in naive snails were artificially depolarized (2.0 ± 0.7, see above).

If the depolarization of the CGCs after conditioning were necessary as well as sufficient for the conditioned fictive feeding response, then it should be possible to reverse the effects of conditioning by reversing this depolarization. However, while doing this experiment, we found that artificial somal hyperpolarization was not transmitted efficiently to the axonal processes where the synaptic sites between the CGCs and target neurons in the cerebral ganglia are thought to be located [21], and thus it could not reverse the network effect of conditioning (see Figure S1 in the Supplemental Data available with this article online). This observation indicated that it is the depolarization of CGC axonal regions presynaptic to its targets within the cerebral ganglia that plays the most direct role in the increased response to the CS, and therefore we next turned our attention to changes induced in these regions by somal depolarization.

Depolarization of the CGC Membrane Potential Leads to an Enhanced Postsynaptic Response and an Increase in Presynaptic Axonal Calcium Levels

By using cell-culture techniques combined with electrophysiology, we examined whether artificial depolarization of CGC somatic membrane potential led to changes in the strength of CGC synaptic output. To monitor these changes, we cocultured a CGC with a B1 motoneuron
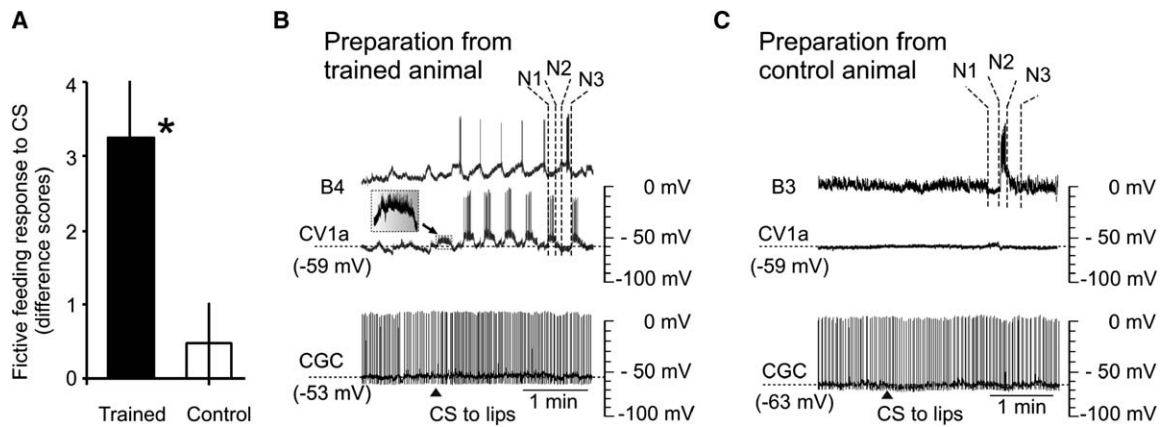
Figure 4. Single-Trial Classical Conditioning Produces Persistent CGC Depolarization and Increases the CS-Induced Fictive Feeding Response

(A) Fictive feeding difference scores of preparations from trained and unpaired control animals. Error bars represent SEM. The computed values for the statistics (unpaired t test) for the difference scores are as follows: df = 18, t = 2.72, p < 0.01. The background fictive feeding activity before the application of the US did not differ significantly (df = 18, p = 0.66) between the trained (1.2 ± 0.6 cycles/2 min) and control (1.6 ± 0.7 cycles/2 min) group. In the same preparations, we found no significant difference in the baseline firing frequencies of CGCs from conditioned versus unpaired control groups (0.83 ± 0.02 and 0.70 ± 0.07 Hz, respectively), nor was there a significant difference in the CS-evoked spike frequency in the two types of preparations (conditioned, 0.84 ± 0.05 Hz; unpaired control, 0.74 ± 0.07 Hz).

(B and C) Examples of recordings from preparations from previously trained and control animals. B3, B4, feeding motoneurons; CV1a, phasically active intrinsic modulatory interneuron; CGC, tonically active extrinsic modulatory interneuron. (B) In a trained preparation, the CS evoked a series of short-latency rhythmic fictive feeding cycles (consisting of phases N1, N2, and N3) with somal spike activity in the appropriate phases in both B4 (N3) and CV1a (N1). In addition, CV1a shows a short-latency burst of blocked axonal spikes or fast subthreshold EPSPs before the full activation of fictive feeding (detail is shown in box at 3× the time and voltage scales of the arrowed section of the CV1a trace). (C) In a control preparation, the CS only evoked a single long-latency cycle of fictive feeding activity, with spike activity in motoneuron B3, but subthreshold in CV1a. Note that the CGC is more depolarized in the trained versus the control preparation (see Results for statistics), but CV1a, unlike the CGC, shows no change in membrane potential after conditioning (mean resting potential in the trained group, −56.5 ± 2.8 mV, n = 9; in the control group, −57.5 ± 3.2 mV, n = 8, unpaired t test, df = 15, t = 0.53, p = 0.6).

(Figure 6A). The CGC is known to be monosynaptically connected to the B1 in the intact CNS [15], and measuring changes in B1 EPSP amplitudes is therefore a convenient assay for the detection of increased CGC synaptic output. The two cells were plated ∼400 μm apart (Figure 6A). This allowed the chemical synaptic connections between the CGC and B1 to be established at about the same distance from the CGC soma where its

axonal branches are thought to synapse onto neurons of the CS pathway in the cerebral ganglia [21] and where calcium imaging was performed in a subsequent experiment (see later). We set the membrane potential of the cultured CGC at different levels with one electrode and triggered single spikes in its soma with a second electrode. We found that although the shape of the CGC spikes did not change as a function of depolarization
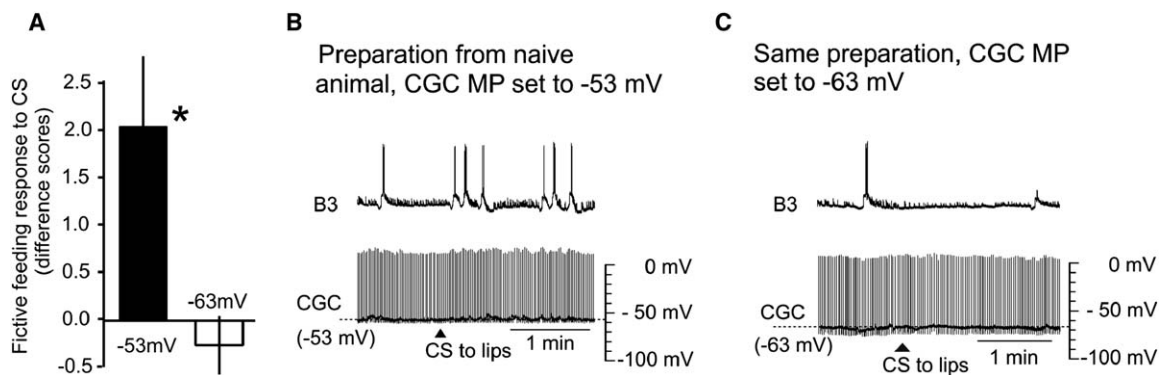
Figure 5. Depolarization of the CGCs in Naive Animals Is Sufficient to Increase CS-Induced Fictive Feeding

(A) Fictive feeding difference scores of preparations from naive animals, in which the CGC membrane potentials were set at either −53 mV or −63 mV, with the CGC firing rates kept at 1 Hz on average (before the 1 Hz entrainment, the firing frequency values in the same CGCs were in the 0.7–1.0 Hz range, similar to the frequency values found in the trained group, see legend to Figure 4). Error bars on the difference score diagrams represent SEM. The computed values for the statistics (paired t test) are as follows: df = 11, t = 2.89, p < 0.01.

(B and C) Examples of electrophysiological recordings from a naive preparation, with the CGCs' membrane potential (MP) set to either −53 mV (B) or −63 mV (C). The firing frequency was similar in both (left and right) CGCs and therefore only one CGC trace is shown in both (B) and (C). At both CGC membrane potential levels, this naive preparation shows some spontaneous fictive feeding activity. However, when the CGC membrane potential is set to −53 mV (B), the CS induces a much stronger response compared to when the MP of the same CGC is set to −63 mV (C), when the CS only induces a delayed subthreshold cycle of synaptic inputs.

A

CGC

B1

B

C
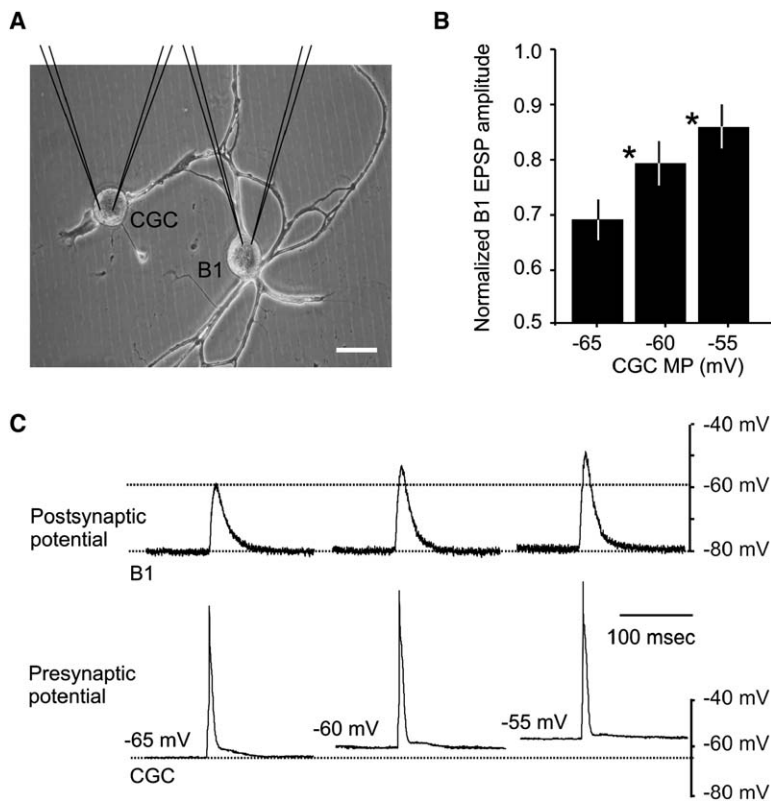
Figure 6. CGC Soma Membrane Depolarization Leads to Increased Postsynaptic Responses

(A) A pair of 3-day-old cocultured CGC and B1 neurons. The superimposed cartoon shows how each of the two neurons was impaled with two electrodes to allow both the setting of the membrane potential at predetermined values in both cells and the triggering of single spikes in the CGCs. Scale bar equals 100 μM.

(B) With increasing soma membrane depolarizations, single spikes triggered in the CGC cell body evoke increasingly larger postsynaptic responses in the cocultured B1 neuron. The CGC membrane potential was increased in 5 mV steps from −65 to −45 mV, and B1 EPSP amplitudes, evoked by single triggered CGC spikes, were measured. This protocol was repeated three times, and after each run the measured amplitude values were normalized to the largest amplitude values (measured at −45 mV in each case). This graph shows the mean normalized B1 EPSP values (±SEM) at the −65, −60, and −55 mV CGC membrane potential levels. The values at both −60 and −55 mV are significantly larger than at −65 mV (paired t tests, df = 2, t = 12.0 and 9.8, p < 0.003 and 0.01).

(C) An example of an electrophysiological test showing increasingly larger postsynaptic responses in the B1 neuron to single spikes triggered in the CGC cell body, which was depolarized in 5 mV steps from −65 to −45 mV. Only the traces in the −65 to −55 mV CGC

membrane potential range are shown. Note that there is no change in the spike shape with increasing levels of depolarization. There are differences in the after-hypolarization in these cultured cell recordings compared with ganglion recordings (Figure 2), but this does not affect our interpretation of the data, which is based on comparisons within the same type of preparation.

(data not shown, example in Figure 6C), the excitatory postsynaptic potentials (EPSPs) in the cocultured and corecorded B1 motoneuron significantly increased in size with increasing presynaptic depolarization (Figures 6B and 6C). Similar results were reported in other invertebrates such as the crayfish neuromuscular synapse and the squid giant synapse [22, 23]. In a separate experiment, we tested whether CGC depolarization could also affect synaptic transmission to the B1 neuron in intact CNS preparations (distance between CGC cell bodies and axonal terminals presynaptic to B1, ∼2 mm), and the results of this experiment are shown in the Supplemental Results.

Recent work in mammalian synapses has shown that depolarization of the presynaptic resting potential increases synaptic output through an elevation of background calcium levels [17]. To test whether there might be a similar mechanism for depolarization-dependent CGC synaptic facilitation, we performed calcium-imaging experiments in various CGC axonal regions in conjunction with depolarization of the voltage-clamped soma membrane in an intact CNS preparation (Figure 7A). We found that a somal depolarization of just 5 mV was already sufficient to induce a small but detectable (≥40 nM) elevation in calcium levels in several sampled axonal regions of the CGC (Figure 7B). A 10 mV voltage step evoked a significantly (p < 0.006) larger calcium response in the same sampled regions (Figure 7B). Moreover, the calcium responses to both the 5 mV and 10 mV somal depolarization were maintained for the duration of

the depolarization, as shown in the examples in Figures 7A and 7C.

Taken together, the above results confirm that control of the membrane potential in the CGC can modulate its synaptic output and suggest that, similarly to mammalian neurons [17], this modulation may be linked to increased presynaptic calcium levels.

Depolarization of the CGC Membrane Potential Increases CS Responses in Feeding Command Neurons

We next sought to determine whether there was a link between somal depolarization of the CGCs and changes at the network level. We therefore performed experiments in naive semi-intact preparations (Figure 1C) with simultaneous intracellular recording of fictive feeding activity in motoneurons, manipulation of CGC membrane potential, and extracellular recording of spike activity in the cerebro-buccal connectives (cbc). We previously showed that chemical conditioning increased the CS response in CBI neurons [24], command-like cerebral-buccal interneurons of the feeding system, which are directly involved in the activation of feeding via their excitatory synaptic connections with the CPG circuitry (Figure 1B). We hypothesized that this short-latency increase in the CS response of CBIs after learning is due to the facilitation of the CS to CBI synaptic pathway by the depolarized CGC (Figure 8A). That this might be the case was also indicated by the observation that in trained preparations where CV1a, a CBI
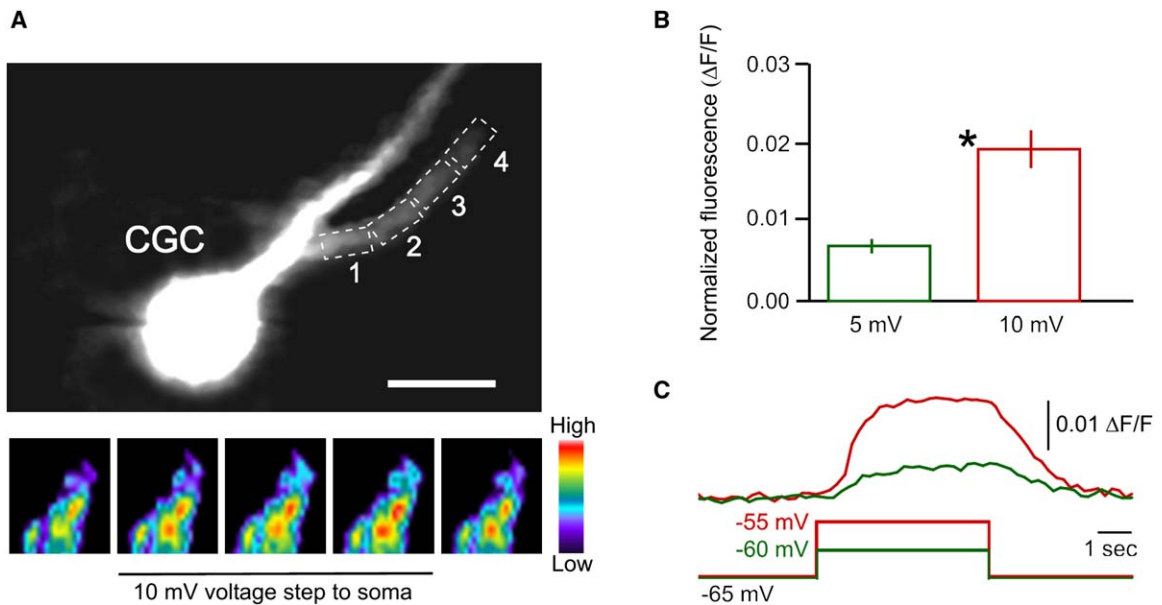
Figure 7. CGC Soma Membrane Depolarization Leads to a Rise in Calcium Levels in Axonal Branches

(A) A CGC filled intracellularly with the calcium-sensitive dye Oregon Green 488 BAPTA-1 and impaled with two electrodes for voltage-clamp experiments. This dye can detect calcium signals with a 40 nM threshold (Molecular Probes Product Information, http://probes.invitrogen.com/media/pis/mp03010.pdf). Scale bar equals 100 μM. Calcium signals were sampled from the four axonal regions shown in the rectangles while the voltage-clamped CGC membrane potential was stepped from −65 mV to −60 mV and −55 mV, respectively. The example sequence shows calcium signals color-coded for intensity (low to high) from axonal region 4 immediately before, during (bar), and immediately after the −65 mV to −55 mV step. The sequence images are magnified 4× compared to the image of the CGC above.

(B) Increases in the strength of the calcium signals sampled in four different axonal regions of the voltage clamped CGC shown in (A), in response to a 5 mV and a 10 mV voltage step from a holding potential of −65 mV. Error bars represent SEM. The normalized fluorescence signal (ΔF/F) is significantly (paired t test, df = 3, t = 7.12, p < 0.006) stronger at 10 mV versus 5 mV, indicating that it is a function of the level of somal depolarization.

(C) Both a 5 mV (green) and a 10 mV (red) voltage step applied to the voltage-clamped CGC soma membrane evokes a maintained calcium signal in axonal region 4.

neuron, was recorded, there was often short-latency CV1a spike activity after the application of the CS (see example in Figure 4B).

We examined the effect of artificial CGC membrane potential depolarization on the CS responses of the CBIs by recording their axonal spikes on the cerebro-buccal connective by using en passant electrodes. This allowed us to monitor population spike responses to the CS in the CBIs that project to the buccal ganglia via the cerebro-buccal connective (cf. [24]). CGCs in naive preparations (n = 5) were depolarized by 10 mV from the nonmanipulated ("recorded") membrane potential (mean, 61.2 ± 4.7 mV) while keeping their firing rate constant and the CBI population response compared in the same preparations with the CGCs at recorded membrane potential.

When the CGC was depolarized, the average increase in CBI spike activity in the first 10 s after CS application, before the activation of fictive feeding, was significantly (p < 0.04) greater (18 ± 5 spikes/bin) compared with the change when the CGC was at the recorded membrane potential (2 ± 3 spikes/bin) (Figure 8B). The same was true for CS-induced CBI activity measured during the entire period of the application of the CS (30 s) (df = 4, t = 3.20, p < 0.03, data not shown). The baseline CBI population activity was not significantly different at the two different CGC membrane potentials (32 ± 3 spikes/bin at the recorded membrane potential compared with 26 ± 5 spikes/bin at the depolarized membrane potential,

paired t test, df = 4, t = 1.68, p = 0.17). Figures 8C and 8D show examples of simultaneous recordings from the cerebro-buccal connective, CGC, B4, and B1 motoneurons in the same preparation, with the CGC at recorded membrane potential (Figure 8C) or depolarized (Figure 8D). The top traces in Figures 8C and 8D show the number of CBI spikes in 1 s bins in a ∼30 s period before and after the application of the CS to the lips. The background CBI activity was similar at the two different CGC membrane potential levels, but there was a rapid and marked increase in the number of extracellularly recorded CS-evoked CBI spikes when the CGC was depolarized, which was absent when the CGC was at recorded membrane potential. When the CGC was depolarized, the initial increase in CBI activity was followed by a CPG-driven fictive feeding cycle monitored here in the B4 and B1 motoneurons (Figure 8D). In contrast, when the CGC was at recorded membrane potential, fictive feeding was not activated by the CS (Figure 8C).

Taken together, the above results suggest that CGC depolarization increases CBI responses to the CS, providing a powerful network-level mechanism for enabling the activation of feeding by the CS after behavioral conditioning.

Discussion

We showed here that an important extrinsic modulatory interneuron of a molluscan feeding system developed
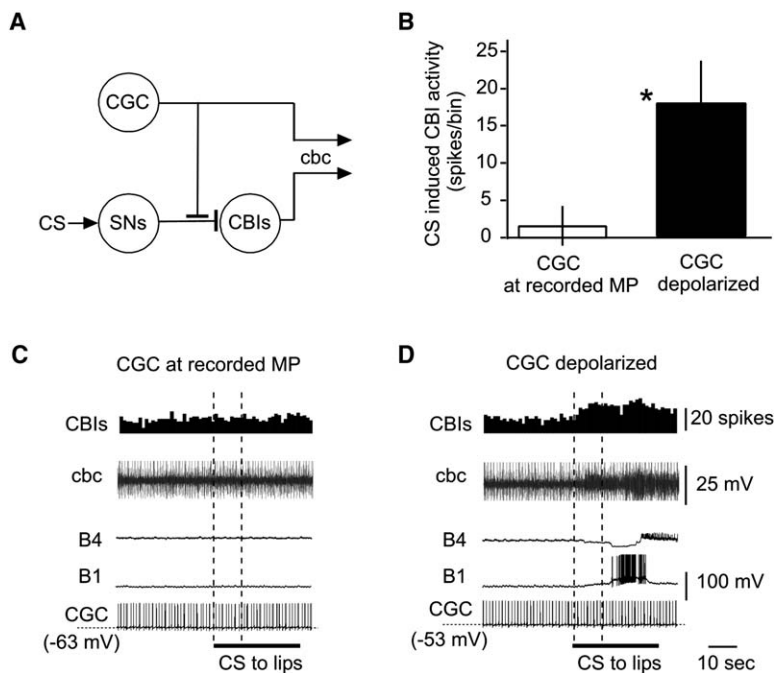
Figure 8. CGC Soma Membrane Depolarization Increases CS-Activated Cerebral-Buccal Interneuron Spike Activity

(A) A diagram of the postulated excitatory synaptic connection between the CGC and sensory neurons (SN) of the CS pathway. The CS pathway provides excitatory synaptic inputs to the cerebral-buccal interneurons (CBIs). The CBIs are the only neurons that project from the cerebral to the buccal ganglia and they were identified by conjoint extracellular recording from the cerebro-buccal connectives (cbc-s) and intracellular recordings from individual CBIs [27]. Previous work [24] showed that the frequency of extracellular units later identified as CBI spikes [27] increases after single-trial chemical conditioning. Graded voltage changes in the soma need to spread in the CGC axon far enough to affect the SN to CBI synaptic pathway.

(B) The CS-evoked increase in the number of CBI spikes in the first 10 s after application is significantly larger when the CGC is depolarized compared with when it is at recorded membrane potential (MP). The data shown here are the means (±SEM) of the number of spikes counted in 1 s bins. The computed values for the statistics (paired t test) are as follows: $df = 4$, $t = 2.95$, $p < 0.04$.

(C) The lack of CS-induced effects on CBI activity and fictive feeding in a naive preparation with the CGC at recorded membrane potential.

(D) CS-induced increase in CBI activity (binned spike diagrams and cbc traces) and fictive feeding (B1 and B4 traces) in the same preparation as in (C), but with the CGC depolarized by 10 mV. The CGC spikes in the cbc trace are cropped. The B1 motoneuron starts firing full-size spikes in the N1 phase of fictive feeding, ~15 s after the application of the CS. The B4 motoneuron is inhibited in the N1 and N2 phases and fires axonal spikes in the N3 phase. The dashed lines indicate the 10 s time intervals after the application of the CS during which CBI spike data were compared (see [B]).

a delayed persistent depolarization after classical food-reward conditioning. Extensive recording of the CGCs with other feeding neurons [6, 13–16, 21] has excluded the possibility that the CGC depolarization is indirect and due to electrotonic coupling. We also showed that this experience-induced nonsynaptic plasticity encodes information that enables the expression of long-term associative memory and described mechanisms by which this information can be translated into modified network and behavioral output.

The use of a single-trial protocol allowed us to follow both the onset and persistence of neuronal changes that paralleled the time course of long-term memory and could therefore contribute to it specifically. The depolarization of the CGCs emerged between 16 and 24 hr posttraining and lasted as long as the behavioral and electrophysiological memory trace was followed. The delayed onset of the depolarization of the CGC shows that it is not involved in the early expression of the memory trace or any consolidation process taking place between 2 and 16 hr posttraining, suggesting that this delayed nonsynaptic plasticity is involved in long-term memory only. A contribution of this depolarization to the long-term memory trace is indicated by the evidence that artificial depolarization of the CGCs in naive snails increases the responsiveness of the entire feeding network to the CS.

While long-term memory may be supported by the depolarized state of the CGCs, early memory and memory consolidation must involve other mechanisms, e.g., synaptic plasticity in the CGCs or synaptic and nonsynaptic plasticity in neurons intrinsic to the rhythmic feeding network. Previous work on *Lymnaea* has described

plastic changes in the synaptic connections of the CGCs with feeding central pattern generator interneurons and motoneurons, resulting either from aversive conditioning [25] or injection with cAMP or PKA [26], and it is reasonable to assume that synaptic changes in the CGCs and/or other neurons also occur after reward conditioning. If these synaptic changes also persist in parallel with long-term memory, the role of the learning-induced membrane potential depolarization of the CGCs may be to add a type of extrinsic nonsynaptic plasticity to the feeding circuit to support long-term memory. Thus, persistent nonsynaptic plasticity can serve as a backup for the effects of learning-induced synaptic plasticity as proposed by [3]. It can also support the consolidated memory trace by itself, as demonstrated by our artificial CGC depolarization experiments in naive snails (Figure 5), indicating that it may also have a significant effect even in the absence of synaptic plasticity.

The neuronal mechanisms of the persistent conditioning-induced depolarization of the CGC are not yet known in detail. Recent work from our laboratory, however, provided evidence that a previously identified cAMP-responsive persistent sodium current of the CGC soma membrane [27, 28] significantly increases >24 hr after single-trial classical conditioning (E.S.N., unpublished observations). This type of sodium current is known to make an important contribution to the depolarization of the membrane potential and increased responses to subthreshold stimuli in other systems [29–32], and it plays a similar role in the CGC [28]. Other electrical parameters of the CGCs (e.g., input resistance, spike characteristics) remained unchanged after

training. A persistent depolarization with no other electrical changes may seem unusual, but there are a number of other important examples, where depolarization occurs with no or very little underlying change in input resistance or spike characteristics [6, 33–36]. It also has been shown that experience-induced presynaptic depolarization can lead to significant postsynaptic and network effects in the absence of other electrical changes usually associated with increased excitability [6, 17, 35].

At the network level, we showed that depolarization of the CGCs enabled the input arising from the conditioned stimulus to activate feeding. Thus, we propose that learning-induced persistent CGC depolarization results in the functional strengthening of CS chemosensory processing pathways through an enhanced modulation of sensory cell to command neuron synapses (Figure 8A).

The cellular mechanism of the translation of CGC depolarization into modified network output is most likely based on the observed effects of somal depolarization on the axonal branches of the CGC presynaptic to the CS sensory pathways. Recent work has shown that small depolarizations of the membrane potential of mammalian neurons (by ∼10 mV, same as the learning-induced change in the CGCs), which do not result in changes in spike size and shape, elicit small calcium currents in the presynaptic terminals [17]. These currents had no measurable effect on the electrical properties of the presynaptic membrane but were sufficient to enhance the probability of spike-induced transmitter release up to 2-fold and lead to a significant enhancement of postsynaptic potentials. We showed here (Figure 7) that a 10 mV (or even a 5 mV) somal depolarization can similarly increase calcium influx into presynaptic axonal regions of the CGCs and also enhance the postsynaptic effects of CGC spikes (Figure 6). Our results on depolarization-induced changes in calcium levels and synaptic output are, however, only suggestive of the persistent cellular changes resulting from conditioning. For example, an important issue is the mechanism of long-term maintenance of increased background calcium levels in the persistently depolarized CGCs of the conditioned animals. Noninactivating calcium channels have been found in molluscan neuronal cell bodies, and these could result in steady increases in calcium levels despite intracellular buffering [37]. A previous voltage-clamp study [27] did not find a persistent calcium current in the CGC soma, but the maintained increase in the axonal calcium signal could be due to release from intracellular calcium stores in the axonal compartment or to the selective expression of noninactivating calcium channels in axons (not detectable with somal voltage-clamp recording).

This work in the CGCs contrasts with our previous study that used multitrial tactile conditioning, where depolarization occurred in a modulatory neuron intrinsic to the feeding circuitry [6], but not in the CGC. Conversely, the same intrinsic modulatory neuron, CV1a, did not show a persistent depolarization after single-trial chemical conditioning (Figure 4B). It seems therefore that the same type of nonsynaptic plasticity but in different types of neurons may be the substrate for memory formation after different classical conditioning procedures, sharing the same US (sucrose) but paired with different types of CS (tactile and chemical).

Previous work on the cellular mechanisms of classical conditioning (resulting in implicit memory [38, 39]) identified experience-induced changes in neurons that are intrinsic to the network responsible for the generation of the conditioned behavior [5, 6, 30, 40–50], including an example of a serotonergic neuron in *C. elegans* [51]. Our new work, however, provides the first example where a persistent experience-induced electrical change in a neuron that lies outside the main mechanism for the generation of a learned motor behavior encodes information that can be used for the recall of an implicit memory trace. The storage of memory-related information outside the network that is strongly activated during rhythmic feeding behavior and also can be spontaneously active [10, 52] may provide a mechanism that prevents extinction due to the motor pattern occurring repeatedly in the absence of the CS. The existence of such an independent back-up mechanism may be particularly important for maintaining robust long-term memory after single-trial conditioning.

Experimental Procedures

Experimental Animals
Groups of animals from a laboratory-bred stock of *Lymnaea stagnalis* were used in the experiments, with details of their maintenance described in the Supplemental Experimental Procedures.

One-Trial Conditioning Protocol
Appetitive chemical classical conditioning of intact animals was carried out via a method based on a previously described single-trial reward classical conditioning protocol [19, 20]. The conditioning experiments and memory tests are described in more detail in the Supplemental Experimental Procedures.

Systems Description and Electrophysiology
The paired CGC neurons (location and anatomy in Figure 1A) were routinely recorded in semi-intact preparations (Figure 1C), together with one or two feeding motoneurons to monitor background and CS-evoked fictive feeding. In some experiments, the CV1a (cerebroventral 1a) cells were also recorded. A detailed explanation of the choice of neurons to be recorded, description of preparations, stimulation and recording protocols, and data analysis methods are described in the Supplemental Experimental Procedures.

Optical Recording of CGC Activity
The optical recording of the CGC electrical activity (Figures S1C and S1D) was performed with the fast-response voltage-sensitive dye JPW-1114 (Molecular Probes, Eugene, OR). This dye was reported to be suitable to monitor the voltage changes in neurites of molluscan neurons [53]. We used this method to measure the spread of somal hyperpolarization of the CGC to the axonal domain. Technical details of this experiment are provided in the Supplemental Experimental Procedures.

Calcium Imaging
For calcium imaging (Figure 7), we used the calcium-sensitive dye Oregon Green 488 BAPTA 1 (Molecular Probes). We used calcium imaging to measure changes in calcium influx in the axonal domain of the CGC in response to somal depolarization. These experiments are described in detail in the Supplemental Experimental Procedures.

Isolation of the CGC and B1 for Electrophysiological Analysis in Culture
Our cell-culture procedure has been described in detail elsewhere [16, 28] and it is briefly described in the Supplemental Experimental Procedures.

Statistical Methods

The behavioral and electrophysiological data from experimental and control animals or preparations were analyzed as described previously [6, 18, 20, 24]. Within-group comparisons were made by paired t tests, while for between-group comparisons, we used unpaired t tests. Differences were considered significant when p < 0.05.

Supplemental Data

Supplemental Data include one figure, Supplemental Results, and Supplemental Experimental Procedures and can be found with this article online at http://www.current-biology.com/cgi/content/full/16/13/1269/DC1/.

References

1. Giese, K.P., Peters, M., and Vernon, J. (2001). Modulation of excitability as a learning and memory mechanism: a molecular genetic perspective. Physiol. Behav. 73, 803–810.
2. Debanne, D., Daoudal, G., Sourdet, V., and Russier, M. (2003). Brain plasticity and ion channels. J. Physiol. (Paris) 97, 403–414.
3. Zhang, W., and Linden, D.J. (2003). The other side of the engram: experience-driven changes in neuronal intrinsic excitability. Nat. Rev. Neurosci. 4, 885–900.
4. Magee, J.C., and Johnston, D. (2005). Plasticity of dendritic function. Curr. Opin. Neurobiol. 15, 334–342.
5. Brembs, B., Lorenzetti, F.D., Reyes, F.D., Baxter, D.A., and Byrne, J.H. (2002). Operant reward learning in Aplysia: neuronal correlates and mechanisms. Science 296, 1706–1709.
6. Jones, N.G., Kemenes, I., Kemenes, G., and Benjamin, P.R. (2003). A persistent cellular change in a single modulatory neuron contributes to associative long-term memory. Curr. Biol. 13, 1064–1069.
7. Lorenzetti, F.D., Mozzachiodi, R., Baxter, D.A., and Byrne, J.H. (2006). Classical and operant conditioning differentially modify the intrinsic properties of an identified neuron. Nat. Neurosci. 9, 17–19.
8. Evans, C.G., and Cropper, E.C. (1998). Proprioceptive input to feeding motor programs in Aplysia. J. Neurosci. 18, 8016–8031.
9. McCrohan, C.R., and Benjamin, P.R. (1980). Patterns of activity and axonal projections of the cerebral giant cells of the snail, Lymnaea stagnalis. J. Exp. Biol. 85, 149–168.
10. Kemenes, G., Staras, K., and Benjamin, P.R. (2001). Multiple types of control by identified interneurons in a sensory-activated rhythmic motor pattern. J. Neurosci. 21, 2903–2911.
11. Plummer, M.R., and Kirk, M.D. (1990). Premotor neurons B51 and B52 in the buccal ganglia of Aplysia californica: synaptic connections, effects on ongoing motor rhythms, and peptide modulation. J. Neurophysiol. 63, 539–558.
12. Kupfermann, I., and Weiss, K.R. (1982). Activity of an identified serotonergic neuron in free moving Aplysia correlates with behavioral arousal. Brain Res. 241, 334–337.
13. Yeoman, M.S., Kemenes, G., Benjamin, P.R., and Elliott, C.J. (1994). Modulatory role for the serotonergic cerebral giant cells in the feeding system of the snail, Lymnaea. II. Photoinactivation. J. Neurophysiol. 72, 1372–1382.
14. Yeoman, M.S., Pieneman, A.W., Ferguson, G.P., Ter Maat, A., and Benjamin, P.R. (1994). Modulatory role for the serotonergic cerebral giant cells in the feeding system of the snail, Lymnaea. I. Fine wire recording in the intact animal and pharmacology. J. Neurophysiol. 72, 1357–1371.
15. McCrohan, C.R., and Benjamin, P.R. (1980). Synaptic relationships of the cerebral giant cells with motoneurones in the feeding system of Lymnaea stagnalis. J. Exp. Biol. 85, 169–186.
16. Straub, V.A., and Benjamin, P.R. (2001). Extrinsic modulation and motor pattern generation in a feeding network: a cellular study. J. Neurosci. 21, 1767–1778.
17. Awatramani, G.B., Price, G.D., and Trussell, L.O. (2005). Modulation of transmitter release by presynaptic resting potential and background calcium levels. Neuron 48, 109–121.
18. Fulton, D., Kemenes, I., Andrew, R.J., and Benjamin, P.R. (2005). A single time-window for protein synthesis-dependent long-term memory formation after one-trial appetitive conditioning. Eur. J. Neurosci. 21, 1347–1358.
19. Alexander, J.E., Audesirk, T.E., and Audesirk, G.J. (1984). One-trial reward learning in the snail Lymnaea stagnalis. J. Neurobiol. 15, 67–72.
20. Kemenes, I., Kemenes, G., Andrew, R.J., Benjamin, P.R., and O'Shea, M. (2002). Critical time-window for NO-cGMP-dependent long-term memory formation after one-trial appetitive conditioning. J. Neurosci. 22, 1414–1425.
21. Styles, B. (2004). Learning and sensory processing in a simple brain. PhD thesis, University of Sussex, Brighton, East Sussex, United Kingdom.
22. Charlton, M.P., and Atwood, H.L. (1977). Modulation of transmitter release by intracellular sodium in squid giant synapse. Brain Res. 134, 367–371.
23. Wojtowicz, J.M., and Atwood, H.L. (1984). Presynaptic membrane potential and transmitter release at the crayfish neuromuscular junction. J. Neurophysiol. 52, 99–113.
24. Straub, V.A., Styles, B.J., Ireland, J.S., O'Shea, M., and Benjamin, P.R. (2004). Central localization of plasticity involved in appetitive conditioning in Lymnaea. Learn. Mem. 11, 787–793.
25. Kojima, S., Nanakamura, H., Nagayama, S., Fujito, Y., and Ito, E. (1997). Enhancement of an inhibitory input to the feeding central pattern generator in Lymnaea stagnalis during conditioned taste-aversion learning. Neurosci. Lett. 230, 179–182.
26. Nakamura, H., Kobayashi, S., Kojima, S., Urano, A., and Ito, E. (1999). PKA-dependent regulation of synaptic enhancement between buccal motor neurons and its regulatory interneuron in Lymnaea stagnalis. Zool. Sci. 16, 387–394.
27. Staras, K., Gyori, J., and Kemenes, G. (2002). Voltage-gated ionic currents in an identified modulatory cell type controlling molluscan feeding. Eur. J. Neurosci. 15, 109–119.
28. Nikitin, E.S., Kiss, T., Staras, K., O'Shea, M., Benjamin, P.R., and Kemenes, G. (2006). Persistent sodium current is a target for cAMP-induced neuronal plasticity in a state-setting modulatory interneuron. J. Neurophysiol. 95, 453–463.
29. Herzog, R.I., Cummins, T.R., and Waxman, S.G. (2001). Persistent TTX-resistant Na+ current affects resting potential and response to depolarization in simulated spinal sensory neurons. J. Neurophysiol. 86, 1351–1364.
30. Darbon, P., Yvon, C., Legrand, J.C., and Streit, J. (2004). INaP underlies intrinsic spiking and rhythm generation in networks of cultured rat spinal cord neurons. Eur. J. Neurosci. 20, 976–988.
31. Timofeev, I., Grenier, F., and Steriade, M. (2004). Contribution of intrinsic neuronal factors in the generation of cortically driven electrographic seizures. J. Neurophysiol. 92, 1133–1143.
32. Kononenko, N.I., Medina, I., and Dudek, F.E. (2004). Persistent subthreshold voltage-dependent cation single channels in suprachiasmatic nucleus neurons. Neuroscience 129, 85–92.
33. Swandulla, D., and Lux, H.D. (1984). Changes in ionic conductances induced by cAMP in Helix neurons. Brain Res. 305, 115–122.
34. Kemenes, G., Rozsa, K.S., Stefano, G., and Carpenter, D.O. (1992). Distinct receptors for Leu- and Met-enkephalin on the metacerebral giant cell of Aplysia. Cell. Mol. Neurobiol. 12, 107–119.
35. Ross, S.T., and Soltesz, I. (2001). Long-term plasticity in interneurons of the dentate gyrus. Proc. Natl. Acad. Sci. USA 98, 8874–8879.
36. Him, A., and Dutia, M.B. (2001). Intrinsic excitability changes in vestibular nucleus neurons after unilateral deafferentation. Brain Res. 908, 58–66.
37. Kits, K.S., and Mansvelder, H.D. (1996). Voltage gated calcium channels in molluscs: classification, Ca2+ dependent inactivation, modulation and functional roles. Invert. Neurosci. 2, 9–34.

38. Milner, B., Squire, L.R., and Kandel, E.R. (1998). Cognitive neuroscience and the study of memory. Neuron *20*, 445–468.

39. Thompson, R.F. (2005). In search of memory traces. Annu. Rev. Psychol. *56*, 1–23.

40. Hawkins, R.D., Castellucci, V.F., and Kandel, E.R. (1981). Interneurons involved in mediation and modulation of gill-withdrawal reflex in *Aplysia*. I. Identification and characterization. J. Neurophysiol. *45*, 304–314.

41. Hawkins, R.D., and Schacher, S. (1989). Identified facilitator neurons L29 and L28 are excited by cutaneous stimuli used in dishabituation, sensitization, and classical conditioning of *Aplysia*. J. Neurosci. *9*, 4236–4245.

42. Gainutdinov, K.L., Chekmarev, L.J., and Gainutdinova, T.H. (1998). Excitability increase in withdrawal interneurons after conditioning in snail. Neuroreport *9*, 517–520.

43. Balaban, P.M., Bravarenko, N.I., Maksimova, O.A., Nikitin, E., Ierusalimsky, V.N., and Zakharov, I.S. (2001). A single serotonergic modulatory cell can mediate reinforcement in the withdrawal network of the terrestrial snail. Neurobiol. Learn. Mem. *75*, 30–50.

44. Davis, W.J., Gillette, R., Kovac, M.P., Croll, R.P., and Matera, E.M. (1983). Organization of synaptic inputs to paracerebral feeding command interneurons of *Pleurobranchaea californica.* III. Modifications induced by experience. J. Neurophysiol. *49*, 1557–1572.

45. Kovac, M.P., Davis, W.J., Matera, E.M., Morielli, A., and Croll, R.P. (1985). Learning: neural analysis in the isolated brain of a previously trained mollusc, *Pleurobranchaea californica*. Brain Res. *331*, 275–284.

46. Spencer, G.E., Syed, N.I., and Lukowiak, K. (1999). Neural changes after operant conditioning of the aerial respiratory behavior in *Lymnaea stagnalis*. J. Neurosci. *19*, 1836–1843.

47. Jones, N., Kemenes, G., and Benjamin, P.R. (2001). Selective expression of electrical correlates of differential appetitive classical conditioning in a feeding network. J. Neurophysiol. *85*, 89–97.

48. Nargeot, R., Baxter, D.A., and Byrne, J.H. (1999). In vitro analog of operant conditioning in *Aplysia*. II. Modifications of the functional dynamics of an identified neuron contribute to motor pattern selection. J. Neurosci. *19*, 2261–2272.

49. Antonov, I., Antonova, I., Kandel, E.R., and Hawkins, R.D. (2003). Activity-dependent presynaptic facilitation and hebbian LTP are both required and interact during classical conditioning in *Aplysia*. Neuron *37*, 135–147.

50. London, J.A., and Gillette, R. (1986). Mechanism for food avoidance learning in the central pattern generator of feeding behavior of *Pleurobranchaea californica*. Proc. Natl. Acad. Sci. USA *83*, 4058–4062.

51. Zhang, Y., Lu, H., and Bargmann, C.I. (2005). Pathogenic bacteria induce aversive olfactory learning in *Caenorhabditis elegans*. Nature *438*, 179–184.

52. Staras, K., Kemenes, I., Benjamin, P.R., and Kemenes, G. (2003). Loss of self-inhibition is a cellular mechanism for episodic rhythmic behavior. Curr. Biol. *13*, 116–124.

53. Antic, S., Wuskell, J.P., Loew, L., and Zecevic, D. (2000). Functional profile of the giant metacerebral neuron of *Helix aspersa*: temporal and spatial dynamics of electrical activity *in situ*. J. Physiol. *527*, 55–69.

54. Staras, K., Kemenes, G., and Benjamin, P.R. (1998). Pattern-generating role for motoneurons in a rhythmically active neuronal network. J. Neurosci. *18*, 3669–3688.